79-4050

An Experimental Study of a Jet Issuing From a Lifting Wing

H. M. McMahon* and D. L. Antani†
Georgia Institute of Technology, Atlanta, Ga.

An experimental program was conducted to determine the behavior of a round tubulent jet issuing from a lifting two-dimensional wing in crossflow. The jet was located at 65% wing chord on an NACA 0021 airfoil fitted with a 30% chord NACA 4415 flap. The flowfield associated with the jet was surveyed extensively with directional pressure probes to determine local velocity vectors and pressures for three different values of lift coefficient at jet effective velocity ratios (square root of the ratio of the jet dynamic pressure to the freestream dynamic pressure) of 4, 6, and 8. Data describing the jet centerline and the path of the contrarotating vortices accompanying the deflected jet are presented and compared with similar data for a round jet issuing from a large flat plate. The spacing and strength of the vortices are calculated using a simple vortex model previously proposed for the flat plate case. The results show that the penetration of the jet and the vortices increases significantly with increasing lift for the range of test parameters covered in the study. The calculated vortex spacing and strength also show an increase with lift.

Nomenclature

c	=	wing chord
C_L	=	lift coefficient based on wing area
C_p	=	pressure coefficient, $(p-p_\infty)/q_\infty$
C_{p_o}	=	stagnation pressure coefficient, $(p_o - p_{o_\infty})/q_\infty$
d_j	=	jet exit diameter
h	=	half-spacing of vortices
p	=	pressure
p_o	=	stagnation pressure
q	=	dynamic pressure
U_v, V_v, W_v	=	velocity components in the vortex coordinate system
V	=	velocity
X, Y, Z	=	Cartesian wind-tunnel coordinate system (see Fig. 3)
X_v, Y_v, Z_v	=	Cartesian vortex coordinate system (see Fig. 3)
α	=	wing angle of attack
Γ	=	strength of a vortex filament
γ	=	$\Gamma/2d_jV_\infty$
δ	=	flap deflection angle, positive when deflected down
ϵ	=	rake pitch angle measured from Z axis, positive clockwise
λ	=	effective velocity ratio, $\lambda^2 = \rho_j V_j^2/\rho_\infty V_\infty^2$
ρ	=	density
Subscripts		
j	=	jet exit plane
∞	=	freestream conditions

Introduction

ONE of the critical flight regimes of a VTOL aircraft is during the transition from vertical to horizontal flight. During this transition, when the weight of the vehicle is being transferred from the thrust of the lifting jet to the lift on the wings, the vehicle suffers lift loss and pitching moment changes, which are caused by a complex interaction between the downward-directed jet flow and the freestream flow. References 1 and 2 give a good summary of this aerodynamic interaction problem.

This problem has received attention from many investigators. Several experiments[3-5] have been conducted with a jet (usually circular) issuing from a large flat plate into a crossflow, with emphasis on the penetration of the jet and the pressure distribution on the flat plate. Theories[6] have been developed to predict these phenomena. More recently, attention has turned to measurements in the wake between the jet plume and the flat plate[7,8] and to studies of the two large contrarotating vortices, which are a dominant feature of the flowfield around the jet.[9] Fearn and Weston[10] have made a complete mapping of the velocity field in and around the jet issuing from a large flat plate, and the results have been used in two different analytical models for predicting the strength of the vortices.

The flat plate case retains the essential flow features of the interaction problem, while eliminating complications, such as pressure gradients and the presence of circulation and trailing vortices, which would be present in the problem of a jet issuing from a finite wing. The jet issuing from a wing into a deflecting stream has not received nearly the detailed study as has the flat plate case. Surface pressure and force measurements on finite wings in the presence of deflected jets have been reported in Refs. 11 and 12. Mikolowsky[13] measured surface pressures and forces on a two-dimensional wing with a clean configuration, that is, the jet plenum chamber was supplied by air piped inside the wing.

The purpose of the present work is to extend the work of Fearn and Weston[10] to a mapping of the velocity field in and around a jet in the presence of circulation, that is, a jet issuing from a lifting two-dimensional wing. This experimental study combines the experimental configuration used by Mikolowsky[13] with the measurement techniques developed by Fearn and Weston.[10] The objective is to compare data from the wing tests with those from the flat plate in order to investigate changes in the velocity field and the vortex strength and location brought about by the presence of the lifting wing. The data should also be useful in helping to formulate analytical models of the wing-jet interaction.

Equipment and Instrumentation

The experiments were conducted in the Georgia Tech 2.74-m (9.0-ft) wind tunnel which has a circular test section. In order to provide two-dimensional flow around the wing

Received Nov. 3, 1977; revision received Oct. 26, 1978.

Index categories: Aerodynamics; Jets, Wakes, and Viscid-Inviscid Flow Interactions.

*Professor, School of Aerospace Engineering. Member AIAA.

†Assistant Research Engineer, School of Aerospace Engineering. Currently, Senior Engineer, Northrop Corp., Hawthorne, Calif. Member AIAA.

model, the test section was modified by installing flat sidewalls (Fig. 1), which gave a model span of 2.18 m (7.17 ft). The wing was mounted on the balance system 25.4 cm (10 in.) above the tunnel centerline.

The two-dimensional wing had an NACA 0021 airfoil section modified such that it had a straight-line contour from the 80% chord station to the trailing edge. The wing had a chord of 39.04 cm (15.37 in.) and was fitted with a transition strip 9.65 mm (0.38 in.) wide centered at 5% chord on both the upper and lower surface.

In previous tests,[13] the wing exhibited incipient stall at $\alpha = 9$ deg at a lift coefficient of 0.80. Accordingly, a flap was fitted to the wing in order to increase the maximum lift coefficient. The flap had an NACA 4415 section with a chord of 11.71 cm (4.61 in.), i.e., 30% of wing chord, and was made from laminated mahogany. The flap was attached to the wing at four locations corresponding to 10 and 26 jet diameters on either side of the wing centerline. The flap was rotated about its leading edge, which was fixed at 0.10% of wing chord behind the wing trailing edge and 4.5% of wing chord below the wing trailing edge.

The jet exit in the wing was 3.81 cm (1.5 in.) in diameter and was located on the wing centerline at the 65% wing chord station. The jet nozzle consisted of a simple bellmouth with a straight extension leading from a plenum chamber inside the wing to the model surface. The jet air was led inside the wing to the plenum chamber and exited from the nozzle extension in a direction perpendicular to the wing chord. The quality of the jet outflow from this configuration has been reported in Ref. 13.

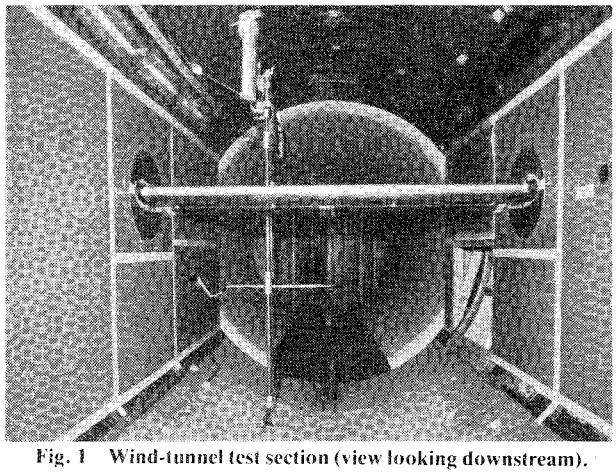

Fig. 1 Wind-tunnel test section (view looking downstream).

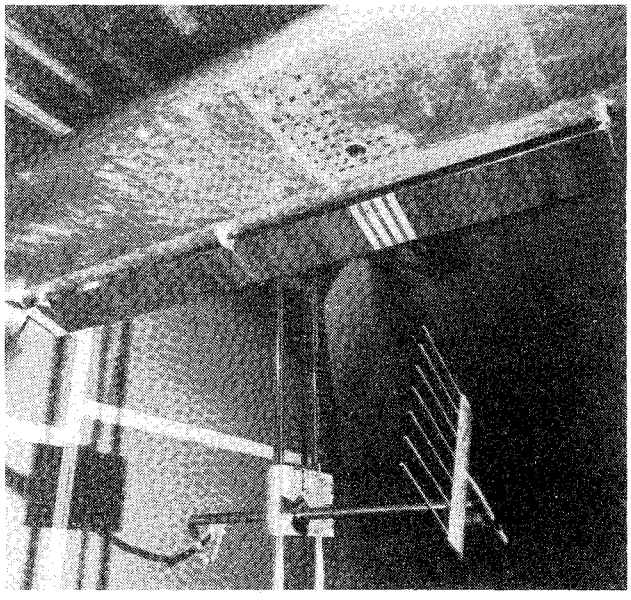

Fig. 2 Model, rake, and actuator.

The velocity in and around the deflected jet was measured with the rake of seven yaw-pitch probes which had been used in previous experiments by Fearn and Weston.[10] Each probe has a hemispherical tip and is 6.35 mm (0.25 in.) in diameter and 20.32 cm (8.0 in.) long, with a 5.08 cm (2.0 in.) spacing between probes. To measure the yaw and pitch angles there are four pressure ports, placed at approximately 45 deg to the total pressure port, in the directions of yaw and pitch. Static pressure was calculated from the measured total, pitch, and yaw pressures. The rake was oriented with the probes arranged vertically, as shown in Fig. 2. The data reduction program for the rake was supplied by NASA Langley Research Center and was verified by preliminary rake tests with the tunnel empty. Only two of the seven probes (the probe at the upper end of the rake and the middle probe), spaced 4 jet diameters apart, were used for taking data.

The rake pressures, the jet plenum chamber stagnation pressure, and the wind-tunnel freestream total and static pressures, were all measured using variable capacitance transducers referenced to ambient pressure. The output of the plenum chamber signal conditioner was monitored on a digital voltmeter. The outputs of all other signal conditioners were read by a computer through a scanner and an integrating voltmeter with a 1/60 s integrating time.

In order to take the required data in the flowfield, it was necessary that the rake be translated in three dimensions in the region downstream of the jet exit. It was also necessary that the rake be rotated in order that the probes were at least approximately aligned with the jet flow, since at large flow angularities the uncertainty in measured flow direction becomes large. The actuator which was designed to meet these requirements is shown in Fig. 2. The vertical and streamwise motion of the actuator, as well as the rotation of the rake, could be manually or computer controlled by sending pulses to appropriate stepping motor drives. Three up-down counters gave a visual display of rake position and pitch angle. The spanwise location of the rake was set manually.

Coordinate Systems

The axis system and nomenclature used in the tests are shown in Fig. 3. The X,Y,Z wind-tunnel coordinate system has its origin at the jet exit on the airfoil surface and not at the wing chordline. This origin moves slightly with wing angle of attack, since the angle of attack was changed by rotating the wing about midchord. Note that the positive Z axis is directed downward. The X_v, Y_v, Z_v coordinate system (with Z_v positive upward) has its origin along the vortex curve, with the Y_v-Z_v plane always being perpendicular to the vortex curve.

Test Conditions and Procedures

All of the experiments were conducted at an indicated freestream velocity of 30.48 m/s (100 ft/s), which corresponds to a Reynolds number (based on wing chord) of 8.15×10^5. Data were taken for three combinations of wing angle of attack and flap deflection angle: $\alpha = 0$ deg, $\delta = -5$ deg

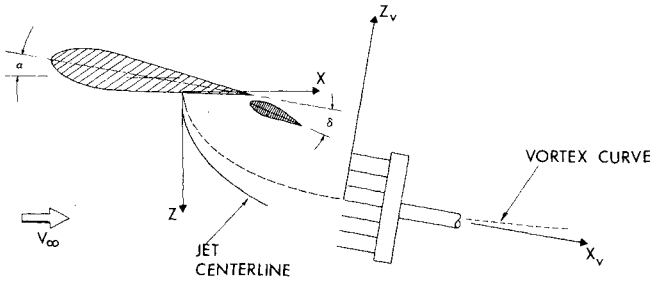

Fig. 3 Axis system and nomenclature.

(minimum lift); $\alpha = 6$ deg, $\delta = 0$ deg (intermediate lift); and $\alpha = 8$ deg, $\delta = 15$ deg (maximum lift). The minimum lift configuration was found by setting the wing at zero angle of attack with the jet off and varying the flap deflection angle until the lift was essentially zero ($C_L = 0.034$). With the wing set at $\alpha = 8$ deg, flap deflection angles of $\delta = 30$ deg and $\delta = 20$ deg led to flow separation over the entire upper surface of the flap. At $\alpha = 8$ deg, $\delta = 15$ deg, centerline surface pressure measurements showed no separation on the upper surface of either the wing or the flap; flow visualization with oil flow on the flap upper surface indicated a separation bubble between about 20% and 30% of flap chord (which was between two surface pressure taps) followed by attached flow to the flap trailing edge. This was considered acceptable; the value of C_L (maximum lift) achieved with the configuration was $C_L = 2.45$. The intermediate lift case was chosen to be about one-half of the maximum lift, and was attained with a convenient combination of $\alpha = 6$ deg, $\delta = 0$ deg.

The effective velocity ratio of the jet λ is defined as $\lambda^2 = q_j/q_\infty$. Data were taken at $\lambda = 4$, 6, and 8. Using a measured value of q_∞, the value of λ desired for a particular test specified the value of q_j. The required plenum stagnation pressure was then calculated assuming that the jet exhausted at an exit pressure p_∞, incorporating a correction factor (obtained from previous calibration[13]) to account for losses in the nozzle.

It was required to measure five pressures from each of the two active probes in the rake. In addition, the freestream total and static pressures were recorded at the start of each rake traverse (i.e., each rake survey along Z_v). A delay of 3 s was used after each rake movement before any probe pressure was measured, and a delay of 2.2 s was used after the step command to the pressure scanners before the pressure at the next scanner port was measured. A traverse of 34 data points typically took 12 min to complete. During many of the traverses there was an overlap in location between one probe and the other, and the repeatability of the calculated velocity components at these points was good.

The actuator system was such that as the rake moved away from the wing centerline it came closer to the rakeholder and vertical guide rods. A preliminary test with a dummy actuator installed in the empty test section showed that the interference effect due to this rake movement was negligible. Comparative measurements of wing surface pressures and forces indicated that installation of the actuator had a negligible interference effect on the wing. After the actuator was installed and carefully aligned, checks on its position and angular accuracy were made. In addition, a record of the initial and final counter readings for each traverse was kept and compared with the required values. It was estimated that, during the taking of the data, the rake position error in X was, at most, ± 1.27 mm (0.05 in.), in Z ± 0.13 mm (0.005 in.), and in rake pitch angle ± 0.3 deg. The Y location of the rake was set manually, with an estimated position error of ± 1.27 mm (0.05 in.).

The pair of contrarotating vortices in the deflected jet induces an upwash in the plane of symmetry ($Y = 0$). The locus of points with maximum induced upwash in the symmetry plane is a measure of the trajectory of the vortex pair. The projection of the vortex trajectories onto the symmetry plane is defined as the vortex curve, and it was desired to take data in planes perpendicular to these vortex curves. As a preliminary step, then, these planes had to be determined. Since there were no available data describing the vortex curve of a jet exhausting from a wing, the empirical vortex curve equation of Fearn and Weston[10] for the flat plate case was used to set up preliminary rake traverses in the plane of symmetry for the wing case. Preliminary traverses were made at five values of X/d_j for the zero and maximum lift cases with $\lambda = 4$ and $\lambda = 8$. These data were plotted as W_v vs Z_v and the locus of points of maximum upwash for each condition was used to determine approximate vortex curves for the jet issuing from the wing. These curves, in turn, were used to define the appropriate angles for the traverses used in the data runs. Since the vortex curves found from the data runs were not greatly different from those used to set up the traverses for the data runs, it was judged to be unnecessary to make a second iteration on the vortex curves. The traverse angles of $\lambda = 6$ and for the intermediate lift case were determined by interpolation.

A computer program was written to control rake movement and the collection of rake data (pressures in the form of voltages). An auxiliary program executed prior to the data runs set up the required Y_v-Z_v planes (i.e., angles ϵ) using the results from the preliminary traverses. The rake was always moved one-half jet diameter along Z_v. The number of steps was specified in the auxiliary program in conjunction with the starting coordinate of the traverse so that the traverse would be centered approximately on the vortex curve. The rake data acquisition program kept the pressure transducers at the most sensitive scale factor possible by first reading each pressure once at a scale factor X1.0, then selecting the appropriate scale factor for the data readings to follow. An average of 25 readings (each integrated over 1/60 s) was taken for each pressure. The output of the data reduction program was a value of U_v, V_v, and W_v (nondimensionalized with the measured V_∞) together with a value of C_{p_o} and C_p for each probe location.

The reduced data from the centerline ($Y = 0$) traverses were used in a plotting program in order to plot W_v vs Z_v and C_{p_o} vs Z_v. The resulting graphs were faired by hand to establish the X-Z location of the maximum value of each quantity. The locus of these maximum points determined the vortex curve and the jet centerline for each test condition.

The strength Γ and the half-spacing of the vortices h were calculated from the velocity measurements using the vortex filament model of Fearn and Weston.[10] In this two-dimensional model, the contrarotating vortices are considered as two straight, infinitely long, vortex filaments placed a distance $2h$ apart. The measured upwash velocities (W_v) from the traverses in the symmetry plane ($Y = 0$) were used to calculate the parameters Γ and h for the filaments. In the model, it is assumed that the component of freestream velocity in the Y_v-Z_v plane is superimposed with that induced by the filaments to give the velocity component which is measured. Thus, the upwash velocity along the Z_v axis is written in terms of the unknown Γ and h as:

$$W_v = \frac{\Gamma h}{\pi (h^2 + Z_v^2)} - V_\infty \sin\epsilon$$

where ϵ is the known angle between the Z and Z_v axes and Z_v is the coordinate with respect to the vortex curve obtained earlier. The strength and the half-spacing were varied[14] to obtain a least-square best fit of the preceding equation to the measured upwash velocities. The root mean square (rms) error for the fit, expressed as a percentage of the maximum upwash velocity measured in the traverse, was calculated to check the quality of the fit.

Results and Discussion

Flowfield

A typical plot of the velocity vector components in a Y_v-Z_v plane is shown in Fig. 4. The flowfield associated with the jet vortex, as well as the vortex location, are readily apparent. Also shown in the figure is the center of the wing-flap wake as determined by examination of the total pressure distribution in the symmetry plane. Note that below the model wake (i.e., below the wing), the flowfield is strongly influenced by the jet. Above the wake, the velocity vectors are essentially the component of the undisturbed freestream velocity in the Y_v-Z_v plane. Thus, there was no significant influence of the jet on the flowfield above the wing-flap wake. The same behavior

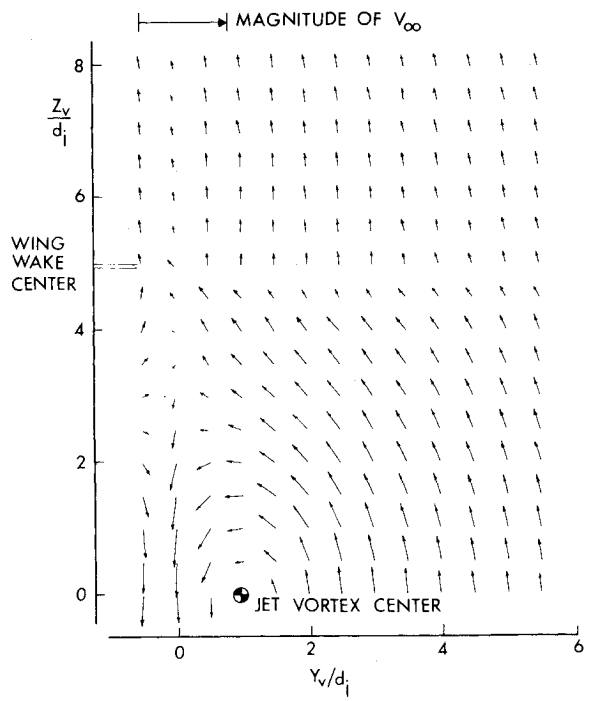

Fig. 4 Typical velocity vectors in Y_v-Z_v plane – $C_L = 0.034$, $\lambda = 4$, $X/d_j = 8$.

was observed at maximum lift at $\lambda = 4$. The traverses at $\lambda = 8$ did not cover the wake region. The magnitude of the vortex spacing and its variation with the various parameters may also be inferred from a series of such vector plots. The symmetry of the flow structure was checked at $Y_v/d_j = -0.5$ with typical results as indicated in Fig. 4.

Jet Centerlines and Vortex Curves

Figure 5 shows the variation of the jet centerline (the locus of points of maximum C_{p_o} in the plane of symmetry $Y = 0$) as a function of C_L and λ. As might be expected from flat plate results, the jet penetrated further into the crossflow with increasing λ at minimum lift. The effect of lift was to increase the penetration of the jet for a given λ and, from the data for $\lambda = 6$, this increase was approximately linear with lift at a constant value of λ. As the lift was increased, the angle that the jet efflux made with the freestream changed from 90-98 deg due to the change in wing angle of attack. However, Eq. (4) of Ref. 15 indicates that such a small change in injection angle has a small influence on the jet penetration and, at the values of X/d_j, shown by the data points in Fig. 5, the penetration due to this effect would, in fact, be slightly reduced. Thus, the change in penetration observed with lift was not caused by the change in jet injection angle. Also shown in Fig. 5 is the empirical equation for the jet centerline as determined in Ref. 10 from experiments with a large flat plate. The maximum difference of one jet diameter between the empirical curves and the present results for minimum lift at all values of λ is not considered significant. What this implies is that there is no significant effect on the jet centerline when an infinite flat plate is replaced by a nonlifting two-dimensional wing of finite chord, even though there is a change in the boundary condition at $Z = 0$ (i.e., removal of the image vortex). It is the downwash in the flowfield due to the lift which has a major effect on the jet centerline and which causes increased jet penetration with lift over that measured for the infinite flat plate case.

Figure 6 shows the behavior of the vortex curves (the projection of the vortex trajectories onto the symmetry plane $Y = 0$) as a function of C_L and λ. Again, as might be expected, at minimum lift the vortex curve moved to increasing values

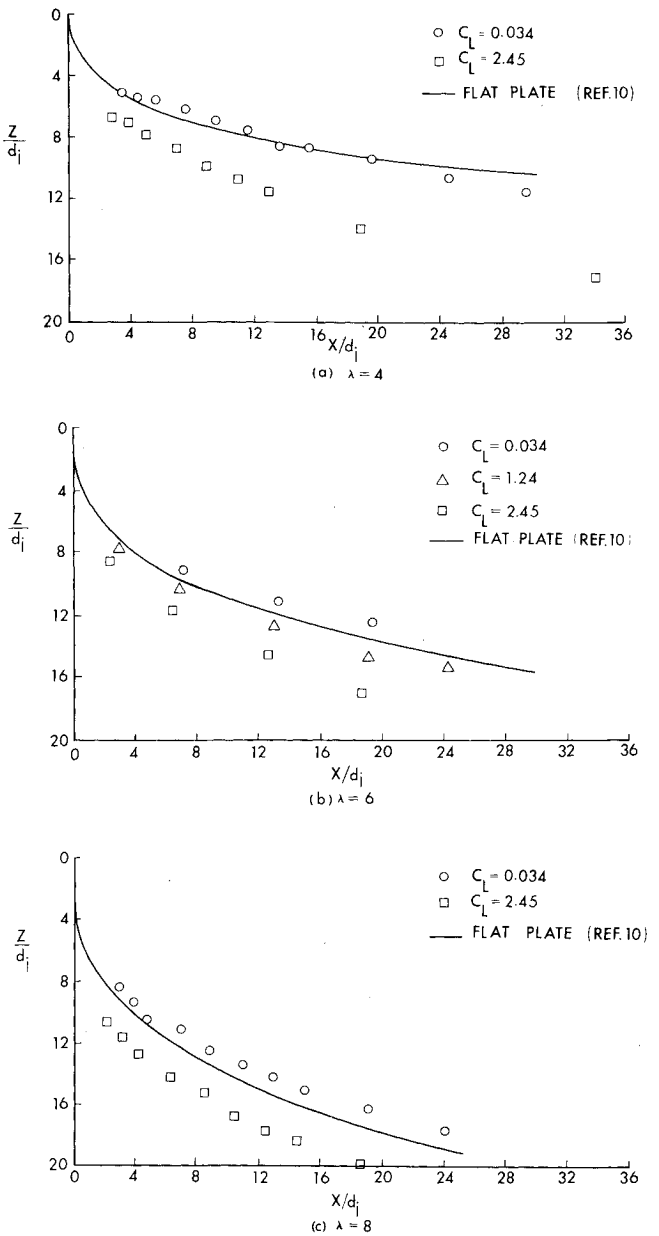

Fig. 5 Variation of jet centerline with lift coefficient.

of Z/d_j as λ increased. The effect of lift was to displace the vortex curve downward for all values of λ and, from the results at $\lambda = 6$, the displacement is linear with C_L for a given λ. The effect of lift, then, was to displace both the jet centerline and the vortex curve downward. However, at $\lambda = 4$ the vertical spacing between the jet centerline and the vortex curve was almost independent of lift; whereas at $\lambda = 8$ the vortex curve was located further above the jet centerline with maximum lift than it was with minimum lift. Thus, the effect of lift on the vortex curve location was less pronounced as λ increased. Also shown in Fig. 6 is the vortex curve empirical equation given in Ref. 10 for the infinite flat plate. The effect on the vortex curve of replacing the flat plate with a body of finite chord at minimum lift is small. Again, as in the case of the jet centerline, the downwash due to lift has a major effect on the vortex curve and displaces it to larger values of Z/d_j than those observed from flat plate experiments.

Vortex Spacing and Strength

Figure 7 shows the nondimensional half-spacing h/d_j between the vortex centers, as calculated from the vortex filament model of Ref. 10. The open data symbols indicate an

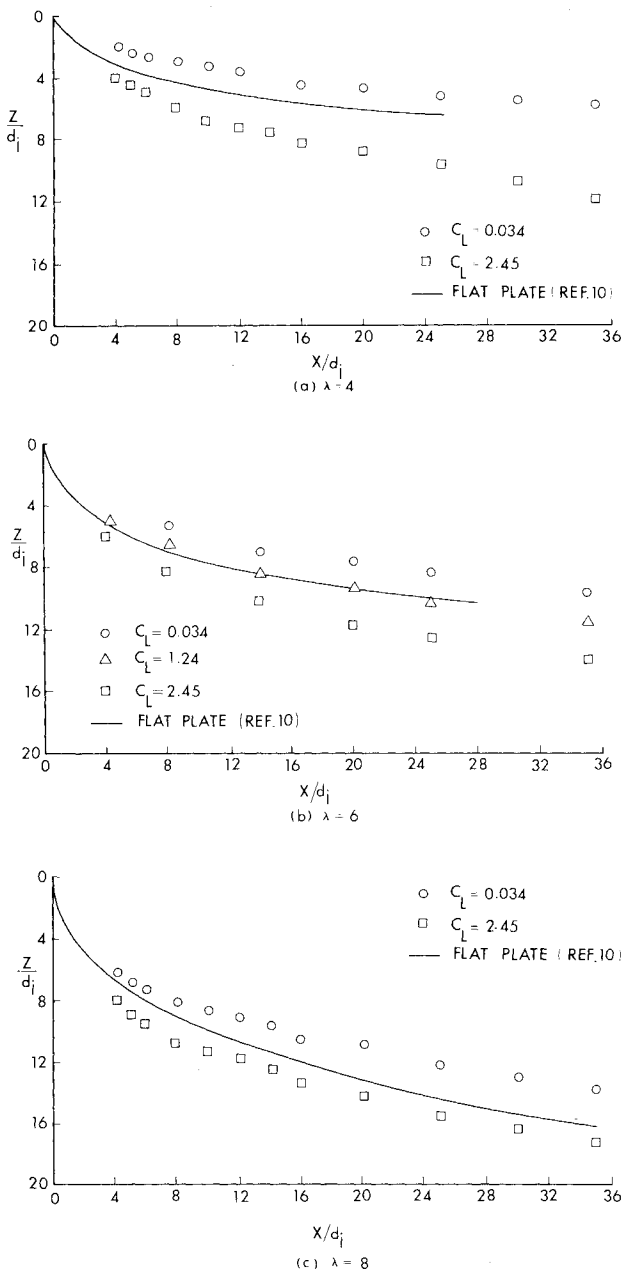

Fig. 6 Variation of vortex curve with lift coefficient.

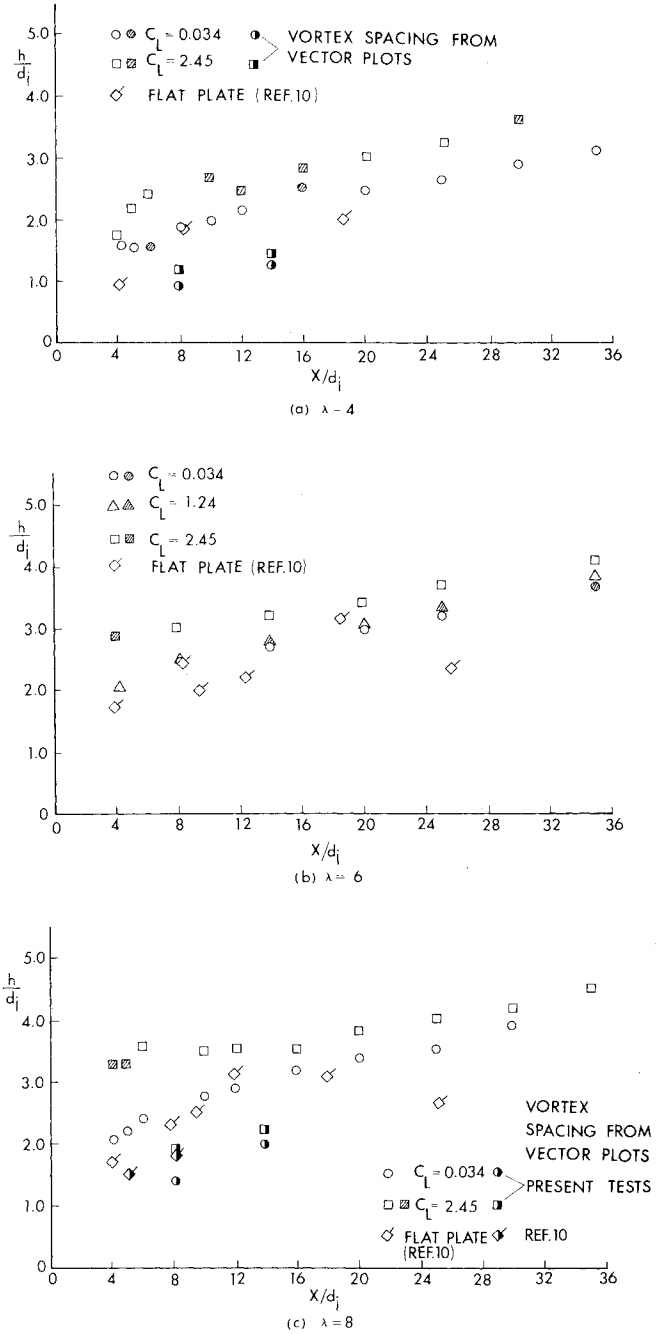

Fig. 7 Variation of vortex spacing with lift coefficient.

rms error of the fit to the measured upwash velocities of $\leq 8\%$ of the maximum W_v/V_∞ measured, and the cross-hatched data symbols indicate an rms error between 8% and a maximum of 16%. The results of this calculation show that, at minimum lift, the half-spacing increased slightly as λ increased (as is also true for the flat plate case) and h increased with increasing X/d_j. The effect of lift was to increase h for all values of λ, with the larger increase occurring for the small values of X/d_j. The results at $\lambda = 6$ indicate that this increase may not be linear with C_L for a given λ. The results for the flat plate, as read from the figures of Ref. 10, are also plotted in Fig. 7, and, at minimum lift, the spacing is slightly higher for the wing than for the flat plate.

Figures 7a and 7c also show the half-spacing of the vortex centers as inferred from vector plots like Fig. 4 and from similar plots presented in Ref. 10. For the flat plate, the half-spacing of the vortices predicted by the filament model tends to be higher (by approximately 20%) than the value for the vortex center half-spacing derived from the vector plots. A similar comparison of the present data shows that the filament model overpredicts the vortex half-spacing by about a factor of two. The filament model computer program used in the calculation of the results from the present tests was checked by using the available data in Ref. 10 for the distribution of W_v/V_∞; the calculated values of h/d_j (and of filament strength) agreed with those reported in Ref. 10. It is not known why the filament model predicts h more accurately for the flat plate case than for the wing case. Since both the vortex strength and the half-spacing are found as unknowns in the least-square fit of the filament model, the values of the vortex strength calculated from the present data may not be of the correct magnitude, but the trends in calculated vortex strength with the parameters of the experiment should still be valid.

Figure 8 shows the nondimensional vortex strength, $\gamma = \Gamma/2d_jV_\infty$, calculated from the filament model as a function of C_L and λ. Again, the open data symbols indicate an rms error of the fit of $\leq 8\%$ of the maximum W_v/V_∞ measured, while the cross-hatched data symbols indicate an rms error between 8% and 16%. The results show that the

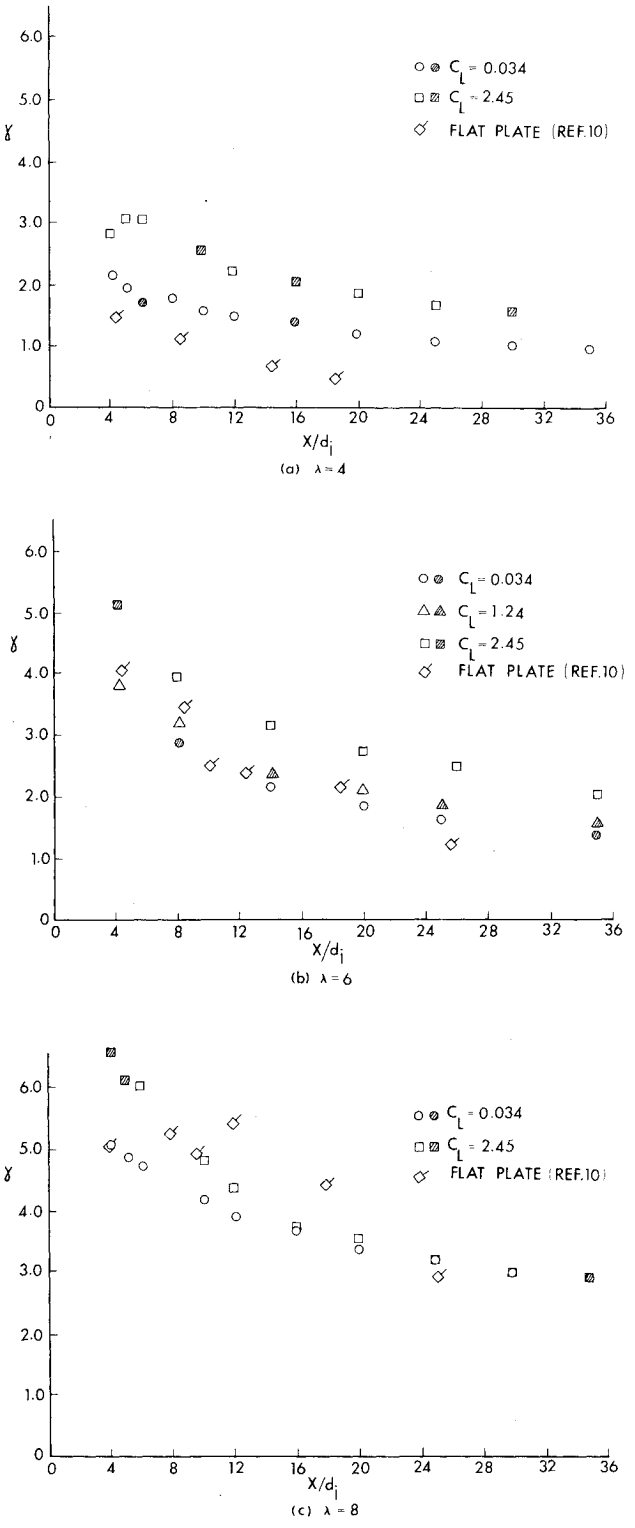

Fig. 8 Variation of vortex strength with lift coefficient.

vortex strength increased with increasing λ at minimum lift. The effect of lift was to increase the vortex strength with increasing C_L, larger increments being evident at lower values of λ. At λ = 8, the increment in strength persisted only up to $X/d_j = 16$. It is believed that the increase in vortex strength with lift is caused primarily by the increase in penetration of the jet with lift. However, this is not certain since at λ = 6 the penetration varied linearly with lift (Fig. 5) while the vortex strength did not.

Examination of Figs. 7 and 8 shows that the trends in γ and h with increasing X/d_j are the same as those observed in the flat plate case,[10] namely that the vortices spread and diffuse such that they gradually weaken one another.

Also plotted in Fig. 8 are the vortex strength values read from the results presented in Ref. 10. The calculated strength at minimum lift using the same filament model is greater than the flat plate values at λ = 4 and less at λ = 8. This comparison with the flat plate may be invalid because of the discrepancy between the half-spacing results discussed earlier. Also, the results for the minimum lift case should not necessarily be expected to agree with the flat plate case, as did the penetration and vortex curve results. There is an interference pressure distribution on the wing due to the jet flow. This interference implies changes in the spanwise loading on the wing even for the minimum lift case. These spanwise changes in circulation away from a constant (two-dimensional) value would imply the shedding of streamwise vorticity from the wing. This vorticity, in turn, may interact with the jet vortex so as to alter its strength even at minimum lift. A more thorough understanding of the effect of lift on the vortex strength can be achieved only after the application of the filament model to the wing case has been resolved.

Conclusions

An experimental investigation of a round turbulent jet issuing from a lifting two-dimensional wing in crossflow gives the following results:

1) The wake of the wing divides the flowfield into two regions at λ = 4. The flowfield in the region below the wake (i.e., the region containing the jet) is strongly influenced by the jet. The flowfield above the wake is not significantly affected by the jet.

2) At approximately zero lift, the penetration of the jet and the location of the vortices are about the same as that observed for a jet issuing from a large flat plate.

3) The jet centerline increases its penetration of the crossflow with increasing lift for all values of λ considered. At λ = 6, the variation with lift is linear.

4) With increasing lift, the vortex curve is displaced in the same direction as the jet centerline. However, the displacement is less at λ = 8 than at λ = 4. At λ = 6, the variation of displacement with lift is linear.

5) The vortex filament model overpredicts the vortex half-spacing compared with that inferred from the velocity vector data. The results using the filament model indicate an increase in vortex spacing with increasing lift at all values of λ.

6) The vortex strength calculated from the filament model increases with increasing lift, with the increase being larger at lower values of λ. At λ = 6, the calculated increase is not linear with lift.

Acknowledgments

This work was supported by NASA under Grant NSG 1257. R. P. Weston of NASA Langley Research Center was the technical officer for this Grant. The authors gratefully acknowledge the assistance of C. Sparrow and J. Craig in the development of the computer software, J. Caudell in the installation and checkout of the instrumentation, and J. Harper, J. Palfrey, and H. Meyer in assisting with the wind-tunnel tests. J. Palfrey also designed the actuator.

References

[1] Margason, R. J. and Fearn, R. L., "Jet-Wake Characteristics and Their Induced Aerodynamic Effects on V/STOL Aircraft in Transitional Flight," NASA SP 218, 1969, pp. 1-18.

[2] Margason, R. L., "Review of Propulsion—Induced Effects on Aerodynamics of Jet/STOL Aircraft," NASA TN D-5617, 1970.

[3] Keffer, J. G. and Baines, W. D., "The Round Turbulent Jet in a Cross Wind," *Journal of Fluid Mechanics*, Vol. 15, Pt. 4, 1963, pp. 481-496.

[4] Bradbury, L. J. S. and Wood, N. M., "The Static Pressure Distribution Around a Circular Jet Exhausting Normally from a

Plane Wall into an Airstream," TN Aero 2978, British Royal Aircraft Establishment, 1964.

[5]Mosher, D. K., "An Experimental Investigation of a Turbulent Jet in a Crossflow," Ph.D. Thesis, Georgia Institute of Technology, Atlanta, Ga., 1970.

[6]Wooler, P.T., "On the Flow Past a Circular Jet Exhausting at Right Angles from a Flat Plate or a Wing," *Journal of the Royal Aeronautical Society*, Vol. 71, March 1967, pp. 216-218.

[7]Kamotani, Y. and Greber, I., "Experiments on a Turbulent Jet in a Cross Flow," *AIAA Journal*, Vol. 10, Nov. 1972, pp. 1425-1492.

[8]Antani, D. L., "An Experimental Investigation of the Vortices and the Wake Associated with a Jet in Crossflow," Ph.D. Thesis, Georgia Institute of Technology, Atlanta, Ga., 1977.

[9]Thompson, A. M., "The Flow Induced by Jets Exhausting Normally from a Plane Wall into an Airstream," Ph.D. Thesis, Univ. of London, 1971.

[10]Fearn, R. and Weston, R. P., "The Vorticity Associated with a Jet in Crossflow," *AIAA Journal*, Vol. 12, Dec. 1974, pp. 1666-1671.

[11]Carter, A., "Effects of Jet-Exhaust Locations on the Longitudinal Aerodynamic Characteristics of a Jet/STOL Model," NASA TN-D-5333, 1969.

[12]Wooler, P. T., Burghart, G. H., and Gallagher, J. T., "The Pressure Distribution on a Rectangular Wing with a Jet Exhausting Normally into an Airstream," *Journal of Aircraft*, Vol. 4, June 1967, pp. 537-543.

[13]Mikolowsky, W. T., "An Experimental Investigation of a Jet Issuing from a Wing in Crossflow," Ph.D. Thesis, Georgia Institute of Technology, Atlanta, Ga., 1972 (University Microfilms #72-26312). A condensed version of the work appears in the *Journal of Aircraft*, Vol. 10, Sept. 1973, pp. 546-553.

[14]Nielsen, K. L., *Methods in Numerical Analysis*, 2nd ed., Macmillan, N.Y., 1964, pp. 308-311.

[15]Margason, R. L., "The Path of a Jet Directed at Large Angles to a Subsonic Free Stream," NASA TN D-4919, 1968.